MNRAS 466, 2939–2947 (2017)
Advance Access publication 2016 December 31
doi:10.1093/mnras/stw3369

A simple and general method for solving detailed chemical evolution with delayed production of iron and other chemical elements

F. Vincenzo,[1,2]★ F. Matteucci[1,2,3] and E. Spitoni[1]

[1] *Dipartimento di Fisica, Sezione di Astronomia, Università di Trieste, via G.B. Tiepolo 11, I-34100 Trieste, Italy*
[2] *INAF, Osservatorio Astronomico di Trieste, via G.B. Tiepolo 11, I-34100 Trieste, Italy*
[3] *INFN, Sezione di Trieste, Via Valerio 2, I-34100 Trieste, Italy*

Accepted 2016 December 23. Received 2016 December 19; in original form 2016 June 22

ABSTRACT

We present a theoretical method for solving the chemical evolution of galaxies by assuming an instantaneous recycling approximation for chemical elements restored by massive stars and the delay time distribution formalism for delayed chemical enrichment by Type Ia Supernovae. The galaxy gas mass assembly history, together with the assumed stellar yields and initial mass function, represents the starting point of this method. We derive a simple and general equation, which closely relates the Laplace transforms of the galaxy gas accretion history and star formation history, which can be used to simplify the problem of retrieving these quantities in the galaxy evolution models assuming a linear Schmidt–Kennicutt law. We find that – once the galaxy star formation history has been reconstructed from our assumptions – the differential equation for the evolution of the chemical element X can be suitably solved with classical methods. We apply our model to reproduce the [O/Fe] and [Si/Fe] versus [Fe/H] chemical abundance patterns as observed at the solar neighbourhood by assuming a decaying exponential infall rate of gas and different delay time distributions for Type Ia Supernovae; we also explore the effect of assuming a non-linear Schmidt–Kennicutt law, with the index of the power law being $k = 1.4$. Although approximate, we conclude that our model with the single-degenerate scenario for Type Ia Supernovae provides the best agreement with the observed set of data. Our method can be used by other complementary galaxy stellar population synthesis models to predict also the chemical evolution of galaxies.

Key words: stars: abundances – ISM: abundances – ISM: evolution – galaxies: abundances – galaxies: evolution.

1 INTRODUCTION

Understanding the evolution of the chemical abundances within the interstellar medium (ISM) of galaxies is fundamental for the development of a galaxy formation and evolution theory that aims at being complete. Numerical codes of chemical evolution address this issue; they can be thought of as a particular realization of stellar population synthesis models, constraining the evolution of galaxies from the perspective of their observed chemical abundance patterns. From a pure theoretical point of view, since the spectral and broad-band photometric properties of stars depend on their initial metallicity, it is clear that the galaxy chemical evolution should be understood first, before drawing the galaxy spectro-photometric evolution.

Chemical evolution models compute the rate of restitution of a given chemical element X, at any time t of galaxy evolution, by taking into account all the stars that die at that time. The latter quantity corresponds to an integral appearing in the differential equations of chemical evolution models, involving the galaxy star formation history (SFH), the initial mass function (IMF) and the nucleosynthetic stellar yields. On the other hand, spectro-photometric models recover the integrated spectrum of a galaxy at any time t of its evolution by taking into account all the stars that are still alive at that time. This quantity is computed by solving two-folded integrals involving the galaxy SFH, the IMF and the stellar spectra.

Given the fact that the integrals involved in chemical and spectro-photometric models are similar, their extremes are complementary: the integrated light from a galaxy is contributed by all the stars that are alive at that time; the chemical elements are mainly contributed (to a first approximation) by all the stars that are dying at that time. The difficulty of building up a fast and accurate chemical evolution model – including chemical elements restored with a certain delay time from the star formation event – to couple with other population synthesis models has represented an obstacle for developing a complete galaxy formation and evolution model for different groups in

★ E-mail: vincenzo@oats.inaf.it

Published by Oxford University Press on behalf of the Royal Astronomical Society

the past. Examples of works combining a chemical evolution model with the galaxy spectro-photometric evolution are those of Brocato et al. (1990), Bressan, Chiosi & Fagotto (1994), Gibson (1997), Silva et al. (1998), Boissier & Prantzos (2000), Calura, Lanfranchi & Matteucci (2008) and Cassarà, Piovan & Chiosi (2015) for unresolved galactic stellar systems and Vincenzo et al. (2016b) for resolved stellar systems.

In this work, we present a simple and fast method to solve chemical evolution of galaxies by assuming an instantaneous recycling approximation (IRA)[1] for chemical elements contributed by massive stars and the delay time distribution (DTD) formalism for chemical elements restored by Type Ia Supernovae (SNe). We aim at reproducing the [α/Fe] versus [Fe/H] chemical abundance patterns as observed in the Milky Way (MW) at the solar neighbourhood by exploring the effect of different prescriptions for the DTD of Type Ia SNe. The assumed galaxy gas mass assembly history represents the starting point of this model. This can be easily incorporated in other stellar population synthesis models to better characterize, in a simple but effective way, the formation and evolution of galaxies from the observed properties of their stellar populations at the present time.

Our work is organized as follows. In Section 2, we present the theoretical framework of our model, namely the main assumptions and the set of differential equations which we solve numerically. In Section 3, we describe the observed set of data for the MW. In Section 4, we present the results of our model, which aims at reproducing the observed [O/Fe] and [Si/Fe] versus [Fe/H] chemical abundance patterns, as observed in the solar neighbourhood. Finally, in Section 5, we end with our conclusions.

2 THEORETICAL FRAMEWORK

Analytical models of chemical evolution have been widely used in the past by theorists and observers to predict the metallicity evolution of a stellar system in a simplified but, at the same time, highly predictive fashion. In fact, although these models have intrinsic shortcomings, they provide a very good approximation for the chemical evolution of elements like oxygen, which are restored on short typical time-scales from the star formation event. Incidentally, oxygen is also the dominant chemical species among the metals in the galaxy ISM, since it is mainly synthesized by massive stars, with lifetimes $\tau \lesssim 30\,\mathrm{Myr}$, dying as core-collapse SNe.

Beyond the metallicity evolution, analytical models of chemical evolution are also able to retrieve the evolution of the galaxy stellar and gas mass with time; therefore, they can draw an approximate but complete physical picture for the evolution of the various galaxy mass components. We remind the reader that the galaxy SFH simply follows from the gas mass evolution, because of the Schmidt–Kennicutt law that is assumed in the models.

Some analytical models do not take into account the fact that the majority of the chemical elements in the ISM usually have more than one nucleosynthesis channel; to further complicate this scenario, each nucleosynthesis channel is also characterized by a distinctive distribution of typical time-scales for the chemical enrichment, which differs from the other.

In this section, we describe our method for solving the problem of coupling different nucleosynthesis channels in analytical chemical evolution models; in particular, we show how the nucleosynthesis from core-collapse SNe can be coupled with the one by Type Ia SNe in a simplified but effective theoretical picture. We think that this method can be useful for both observers and theorists who wish to decouple – for example – the evolution of chemical elements like oxygen and iron, which do not trace each other and are usually used as tracers of the galaxy metallicity.

2.1 The delay time distribution of Type Ia Supernovae

Chemical elements like iron, silicon or calcium are also synthesized by Type Ia SNe beyond core-collapse SNe. It is therefore fundamental to properly take into account the Type Ia SN contribution in a theoretical model of chemical evolution. A useful formalism to compute the Type Ia SN rate in galaxies was developed by Ruiz-Lapuente & Canal (1998) by originally introducing the concept of DTD in the theoretical framework (see also Strolger et al. 2004; Greggio 2005). In this formalism, the Type Ia SN rate is defined as the convolution of the galaxy star formation rate (SFR) with a suitable DTD, as follows.

$$R_{\mathrm{Ia}}(r,t) = C_{\mathrm{Ia}} \int_{\tau_1}^{\min(t,\tau_2)} \mathrm{d}\tau\, \mathrm{DTD}_{\mathrm{Ia}}(\tau)\, \psi(r, t-\tau), \tag{1}$$

where τ_1 and τ_2 are suitable values depending on the adopted scenario for the DTD. The quantity $\psi(t)$ represents the galaxy SFR, with the units $\mathrm{M}_{\odot}\,\mathrm{pc}^{-2}\,\mathrm{Gyr}^{-1}$, and the normalization constant C_{Ia} is related to the fraction of stars in the binary systems giving rise to Type Ia SNe. The function $\mathrm{DTD}_{\mathrm{Ia}}(\tau)$ physically represents the (unnormalized) number of Type Ia SNe, which are expected to explode at the time $t = \tau$ from a burst of star formation at $t = 0$, per unit mass of the simple stellar population (SSP) and per unit time of duration of the burst.

Observational evidence suggests an integrated number of Type Ia SNe, which is ∼1 SN per $M_{\star} = 10^3\,\mathrm{M}_{\odot}$ of the stellar mass formed, with a scatter of about 2–10 around this value (Bell et al. 2003; Maoz, Mannucci & Nelemans 2014). In this work, the normalization constants of the examined DTDs are chosen so as to fulfil this criterion; in particular, the constant C_{Ia} is computed by requiring the following constraint:

$$\frac{\int_{r_1}^{r_2} \mathrm{d}r\, r \int_0^{t_G} \mathrm{d}t'\, R_{\mathrm{Ia}}(r,t')}{\int_{r_1}^{r_2} \mathrm{d}r\, r \int_0^{t_G} \mathrm{d}t'\, \psi(r,t')} = \frac{2\,\mathrm{SNe}}{10^3\,\mathrm{M}_{\odot}}, \tag{2}$$

where r_1 and r_2 are defined as the inner and outer radii, where the integrated number of Type Ia SNe [the numerator in the left-hand side of equation (2)] and the galaxy stellar mass formed (the denominator) are computed.

According to Greggio (2005), the so-called 'double-degenerate scenario' – in which Type Ia SNe originate from binary systems of electron-degenerate CO white dwarfs losing angular momentum via gravitational wave emission – can be modelled by assuming $\mathrm{DTD}_{\mathrm{Ia}}(\tau) \propto 1/\tau$ (see also Totani et al. 2008), which provides almost the same final results for the Type Ia SN rate in galaxies as the DTD proposed by Schönrich & Binney (2009) and recently assumed by Weinberg, Andrews & Freudenburg (2016).

Another widely used DTD often assumed in the literature is the so-called 'bimodal DTD' as determined by Mannucci, Della Valle & Panagia (2006). It was originally defined with the following functional form:

$$\mathrm{DTD}_{\mathrm{Ia}}(\tau) \propto A_1 \exp\left(-\frac{(\tau-\tau')^2}{2\sigma'^2}\right) + A_2 \exp(-\tau/\tau_{\mathrm{D}}), \tag{3}$$

[1] The stellar lifetimes of the stars with mass $m \geq 1\,\mathrm{M}_{\odot}$ are neglected in the differential equations, while they are assumed to be infinite for stars with $m < 1\,\mathrm{M}_{\odot}$.

where the constants $A_1 \approx 19.95$ and $A_2 \approx 0.17$ guarantee that the two terms in the equation equally contribute by 50 per cent; the parameters determining the prompt Gaussian function are $\tau' = 0.05$ Gyr and $\sigma' = 0.01$ Gyr; finally, the time-scale of the tardy declining exponential component is $\tau_{\rm D} = 3$ Gyr.

In this work, we also test the scenario in which Type Ia SNe originate from the C-deflagration of an electron-degenerate CO white dwarf accreting material from a red giant or main-sequence companion (the so-called 'single-degenerate scenario'). We assume for the single-degenerate scenario the same prescriptions as given in Matteucci & Recchi (2001).

2.2 The approximate differential equation for the evolution of a generic chemical element

In this work, we assume IRA for the chemical elements restored by massive stars and the DTD formalism for the delayed chemical enrichment by Type Ia SNe; in particular, we solve the following approximate differential equation for the evolution of the surface gas mass density of a generic chemical element X within the galaxy ISM:

$$\frac{{\rm d}\sigma_X(r,t)}{{\rm d}t} = -X(r,t)\,\psi(r,t) + \hat{\mathcal{E}}_X(r,t) + \hat{\mathcal{O}}_X(r,t) + \hat{\mathcal{R}}_{X,\rm Ia}(r,t), \tag{4}$$

where we assume that the infall gas is of primordial chemical composition. The physical meaning of the various terms in the right-hand side of equation (4) can be summarized as follows.

(i) The first term represents the surface gas mass density of X which is removed per unit time from the galaxy ISM because of the star formation activity. The quantity $X(r, t) = \sigma_X(r, t)/\sigma_{\rm gas}(r, t)$ is the abundance by mass of the chemical element X.

(ii) The second term, $\hat{\mathcal{E}}_X(r,t)$, takes into account both the stellar contributions to the enrichment of the newly formed chemical element X and the unprocessed quantity of X, returned per unit time and surface by dying stars without undergoing any nuclear processing in the stellar interiors. By assuming IRA, one can easily demonstrate that this term can be approximated as follows (Maeder 1992):

$$\hat{\mathcal{E}}_X(r,t) = X(r,t)\,\psi(r,t)\,R + \langle y_X\rangle\,(1-R)\psi(r,t), \tag{5}$$

where the quantity R represents the so-called 'return mass fraction', namely the total mass of gas returned into the ISM by an SSP, per unit mass of the SSP (see also Calura, Ciotti & Nipoti 2014 for a more accurate approximation to compute the gas mass returned by multiple stellar populations), and $\langle y_X\rangle$ is the net yield of X per stellar generation (Tinsley 1980).

(iii) The third term in equation (4) removes the quantity of the chemical element X, which is expelled out of the galaxy potential well because of galactic winds. We assume the galactic wind to be always active over the whole galaxy lifetime and its intensity is directly proportional to the galaxy SFR, namely

$$\hat{O}_X(r,t) = \omega\,\psi(r,t), \tag{6}$$

with ω being the so-called 'mass loading factor', a free parameter in the models. We can also think of the galactic wind as a continuous feedback effect of the SFR, which warms up the galaxy ISM through stellar winds and SN explosions; as a consequence of this, the gas can move from the cold to the hot phase of the ISM, and hence it might not be immediately available for further reprocessing by star formation.

(iv) The fourth term represents the amount of X restored per unit time and surface by Type Ia SNe, where $\langle m_{X,\rm Ia}\rangle$ is the average amount of X synthesized by each single Type Ia SN event. In particular,

$$\hat{\mathcal{R}}_{X,\rm ia}(r,t) = \langle m_{X,\rm Ia}\rangle\;R_{\rm Ia}(r,t), \tag{7}$$

with $R_{\rm Ia}(r, t)$ being the Type Ia SN rate, as defined in equation (1).

In summary, by specifying all the various terms, we can rewrite equation (4) as follows:

$$\frac{{\rm d}\sigma_X(r,t)}{{\rm d}t} = -\sigma_X(r,t)\,\frac{\psi(r,t)}{\sigma_{\rm gas}(r,t)}(1+\omega-R) + \langle y_X\rangle\,(1-R)\,\psi(r,t) + \langle m_{X,\rm Ia}\rangle\,R_{\rm Ia}(r,t). \tag{8}$$

We remark on the fact that equation (8) can be numerically solved with classical methods (e.g. with the Runge–Kutta algorithm), once the SFH of the galaxy has been previously determined, either observationally or theoretically; in Section 2.3, we show how we derive this information. In this work, we solve equation (8) for oxygen, silicon and iron by assuming $\langle y_{\rm O}\rangle = 1.022 \times 10^{-2}$, $\langle y_{\rm Si}\rangle = 8.5 \times 10^{-4}$, $\langle y_{\rm Fe}\rangle = 5.6 \times 10^{-4}$, and $R = 0.285$, which can be obtained by assuming the Kroupa, Tout & Gilmore (1993) IMF (see also Vincenzo et al. 2016a). We adopt the so-called 3/8-rule forth-order Runge–Kutta method to solve equation (8). Finally, we assume the stellar yields of Type Ia SNe from Iwamoto et al. (1999).

2.3 The galaxy star formation history

We test the effect of two distinct phenomenological laws for the SFR: (i) a linear Schmidt–Kennicutt law, as assumed in some analytical and numerical codes of chemical evolution and (ii) a non-linear Schmidt–Kennicutt law. In the first case, the differential equation for the evolution of the galaxy surface gas mass density is linear and it can be easily solved with the Laplace transform method, for any assumed smooth gas mass assembly history, acting in the equation as a source term. In the second case, since the differential equation is non-linear in the unknown, a numerical technique is adopted to solve the problem of retrieving the galaxy SFH.

2.3.1 *Linear Schmidt–Kennicutt law for the galaxy SFR*

In the case of a linear Schmidt–Kennicutt law, the galaxy SFR is assumed to be directly proportional to the galaxy gas mass density, namely

$$\psi(r,t) = \nu_{\rm L}\,\sigma_{\rm gas}(r,t), \tag{9}$$

where $\nu_{\rm L}$ is the so-called 'star formation efficiency', a free parameter in the models, having the units of $\rm Gyr^{-1}$. The galaxy SFH, namely the evolution of the galaxy SFR with time and radius, can be theoretically recovered under IRA by solving the following approximate differential equation for the evolution of the galaxy surface gas mass density:

$$\frac{{\rm d}\sigma_{\rm gas}(r,t)}{{\rm d}t} = -\psi(r,t)(1+\omega-R) + \hat{\mathcal{I}}(r,t). \tag{10}$$

The last term in equation (10) corresponds to the assumed galaxy gas mass assembly history, namely $\hat{\mathcal{I}}(r,t) = ({\rm d}\sigma_{\rm gas}/{\rm d}t)_{\rm inf}$. Most of the chemical evolution models in the literature customarily assume a decaying exponential infall rate of gas with time. Historically, the first work in the literature suggesting such an infall law is the one by Chiosi (1980). Nevertheless, equation (10) can be numerically solved for any assumed galaxy gas accretion history with standard techniques (e.g. a Runge–Kutta algorithm).

If we compute the Laplace transform of equation (10), it is straightforward to verify that the following equation can be obtained:

$$\mathcal{L}(\hat{\mathcal{I}}(r,t))(s) = \frac{s+\alpha}{\nu_{\mathrm{L}}}\,\mathcal{L}(\psi(r,t))(s) - \sigma_{\mathrm{gas}}(r,0), \tag{11}$$

where s is the frequency, with the units of Gyr^{-1}, and $\alpha = (1+\omega-R)\,\nu$. Equation (11) is very general and closely relates the Laplace transform of the galaxy gas accretion history, $\mathcal{L}(I(r,t))(s)$, with the Laplace transform of the galaxy SFH, $\mathcal{L}(\psi(r,t))(s)$, provided the SFR follows a linear Schmidt–Kennicutt law. Equation (11) can be used both to retrieve the galaxy SFH from the assumed gas infall law and to solve the corresponding inverse problem, namely to reconstruct the galaxy gas mass assembly history from the observed SFH [one can assume a fitting function for the galaxy SFH to insert in equation (11)].

By assuming in equation (11) the following law for the galaxy gas mass assembly history:

$$\hat{\mathcal{I}}(r,t) = \sum_j \hat{\mathcal{I}}_j(r,t) = \sum_j A_j(r)\,\mathrm{e}^{-(t-t_j)/\tau_j}\,\Theta(t-t_j), \tag{12}$$

which corresponds to a summation of separate gas accretion episodes, each obeying a decaying exponential law with time-scale τ_j and starting at the time t_j, it is straightforward to verify that the solution for the galaxy SFH is the following:

$$\psi(r,t) = \sum_j \frac{\nu_{\mathrm{L}}\,A_j(r)}{\alpha-\frac{1}{\tau_j}}\,\Theta(t-t_j)[\mathrm{e}^{-(t-t_j)/\tau_j} - \mathrm{e}^{-\alpha(t-t_j)}] + \nu_{\mathrm{L}}\,\sigma_{\mathrm{gas}}(r,0)\,e^{-\alpha t}\,\Theta(t). \tag{13}$$

We remind the reader that the function $\Theta(t)$ in the equations above is defined as the Heaviside step function. Finally, the parameter $A_j(r)$ is a normalization constant, which fixes the total gas mass accreted by the jth accretion episode.

For the sake of simplicity, in this work, we assume the galaxy gas accretion history, as defined in equation (12), to be composed of a single episode, starting at $t = 0$. It can be shown that the functional form for galaxy SFH has the same expression as given in Spitoni, Vincenzo & Matteucci (2016).

It is worth remarking that a linear relation is inferred in galaxies only between the galaxy SFR and the molecular hydrogen surface mass density, $\sigma_{\mathrm{H_2}}$ (Bigiel et al. 2008, 2011; Leroy et al. 2008; Schruba et al. 2011), although the systematic uncertainties in this kind of studies might be still very large to draw firm conclusions. Nevertheless, Kennicutt (1998) noted that the relation between the inferred SFR and the gas mass density, σ_{gas}, can be well fit with a linear law, such as equation (9), when the star formation efficiency is defined as the inverse of the typical dynamical time-scale of the system, following the results of a previous theoretical study by Silk (1997).

2.3.2 *Non-linear Schmidt–Kennicutt law for the galaxy SFR*

In this work, we also test the effect of assuming a non-linear Schmidt–Kennicutt law for the evolution of the galaxy SFR, which has the following form:

$$\psi(r,t) = \mathrm{SFR}_0\left(\frac{\sigma_{\mathrm{gas}}(r,t)}{\sigma_0}\right)^k, \tag{14}$$

where, by following Kennicutt (1998), we assume $k = 1.4$ and $\sigma_0 = 1\,\mathrm{M}_\odot\,\mathrm{pc}^{-2}$; finally, the quantity SFR_0 in equation (14) has the units of a SFR, namely $\mathrm{M}_\odot\,\mathrm{pc}^{-2}\,\mathrm{Gyr}^{-1}$ (see also the discussion below). In our work, we treat the quantity SFR_0 as a free parameter to reproduce the MW chemical abundance patterns.

In the case of a non-linear Schmidt–Kennicutt law, the star formation efficiency varies with radius and time, according to the following equation:

$$\mathrm{SFE}(r,t) = \frac{\psi(r,t)}{\sigma_{\mathrm{gas}}(r,t)} = \frac{\mathrm{SFR}_0}{\sigma_0}\left(\frac{\sigma_{\mathrm{gas}}(r,t)}{\sigma_0}\right)^{k-1}. \tag{15}$$

We remark on the fact that, in the original work by Kennicutt (1998), $\mathrm{SFR}_{0,\,\mathrm{K98}} \approx 2.5\times10^{-1}\,\mathrm{M}_\odot\,\mathrm{pc}^{-2}\,\mathrm{Gyr}^{-1}$, which represents an average quantity, derived by fitting the observed relation between the SFR and σ_{gas} in a sample of nearby star forming galaxies, which exhibit a spread in the SFR–σ_{gas} diagram.

In the physical picture drawn by equation (14), we can argue that – as a consequence of a prolongated and continuous star formation activity, which warms up the galaxy ISM through stellar winds and Type II SNe – the galactic disc likely responds by regulating its dimensions (and hence its global thermodynamical quantities) to saturate towards a level of star formation, which is driven by the quantity SFR_0. In summary, the slope and power law index in equation (14) might represent '*truly basic physical constants*', as pointed out by Talbot & Arnett (1975) almost 40 years ago about the SFR law in the galaxy formation and evolution models.

We are aware that our considerations above are heuristic; in particular, there should be an underlying physical mechanism, common to almost all actively star-forming stellar systems, which is not explained by our simple phenomenological prescriptions for star formation. A detailed physical theory must be developed, involving – for example – physical quantities in a statistical mechanics framework. In particular, one should be able to relate the astronomical quantity 'star formation rate' with many more physical quantities, in order to gain a deeper knowledge about how a small-scale phenomenon like the star formation can be regulated by large-scale processes and vice versa. An interesting attempt to develop a theory for the star formation activity in galaxies can be found in the work by Silk (1997).

In principle, a possible method to solve equations (10) and (14) would be to use the Green functions. In particular, by assuming a non-linear Schmidt-Kennicutt law (equation 14), equation (10) becomes a Bernoulli differential equation with a source function, which is given by the infall term, $\hat{\mathcal{I}}(r,t)$; the corresponding Green function is determined by the response of the system to a Dirac delta function in the infall term, which – as aforementioned – represents the source function in equation (10); hence, from a physical point of view, the Green function corresponds to the solution of the so-called 'closed-box model', with all the gases being already present in the galaxy since the beginning of its evolution.

The exact solution for σ_{gas} with a non-linear Schmidt–Kennicutt law could then be found by convolving the Green function (i.e. the evolution of σ_{gas} in a closed box model, where the equation becomes a Bernoulli differential equation, with no source term) with the assumed gas infall history.

It is worth noting that, if $k = 2$ in equation (14), as expected in the low-density star-forming regions where almost all the gases are in their atomic form (Genzel et al. 2010), then equation (10) for the evolution of σ_{gas} with time can be put in the form of a Riccati equation, which can also be solved analytically.

In summary, we first derive the evolution of $\sigma_{\rm gas}$ with time by solving equation (10) with a numerical algorithm; then, it is straightforward to recover the galaxy SFR by making use of equation (14).

2.4 Free parameters and methods

The free parameters of our model are given by (i) the star formation efficiency, $\nu_{\rm L}$, when the linear Schmidt–Kennicutt law is assumed, or the quantity SFR_0, in the case of a non-linear Schmidt–Kennicutt law; (ii) the mass loading factor, ω, which determines the intensity of the galactic winds and (iii) the infall time-scale, τ, which characterizes the intensity of the gas infall rate, assumed to be a decaying exponential law.

The assumed IMF and the set of stellar yields determine the return mass fraction, R, the net yield of the chemical element X per stellar generation, $\langle y_X \rangle$, and the yield of X from Type Ia SNe, $\langle m_{X,\,\rm Ia} \rangle$. Other fundamental assumptions in the model are given by the DTD for the Type Ia SN rate and the prescription for the SFR law.

An observational constraint for the calibration of the gas infall history is given by the radial profile of the present-day total surface mass density, $\sigma_{\rm tot}(r, t_{\rm G})$, which is very difficult to retrieve from an observational point of view. In this work, we apply our model to reproduce the observed chemical abundance patterns at the solar neighbourhood, where $r_{\rm S} = 8\,\mathrm{kpc}$; hence, we normalize the infall law, as given in equation (12), by requiring the following constraint:

$$\int_0^{t_{\rm G}} \mathrm{d}t\, \hat{\mathcal{I}}(r_{\rm S}, t) = \sigma_{\rm tot}(r_{\rm S}, t_{\rm G}), \tag{16}$$

where we assume $t_{\rm G} = 14\,\mathrm{Gyr}$, a single infall episode, and $\sigma_{\rm tot}(r_{\rm S}, t_{\rm G}) = 54\,\mathrm{M}_{\odot}\,\mathrm{pc}^{-2}$, which represents the present-day total surface mass density at the solar neighbourhood (see also Micali, Matteucci & Romano 2013, which refers to the work by Kuijken & Gilmore 1991).

The best model is defined as the one capable of reproducing the observed trend of the [O/Fe] versus [Fe/H] chemical abundance pattern, which represents the best observational constraint for the chemical evolution models of the MW. Our best models are characterized by the following values of the free parameters:

(i) $\nu_{\rm L} = 2\,\mathrm{Gyr}^{-1}$, for our best model with the linear Schmidt–Kennicutt law, and $\mathrm{SFR}_0 = 2\,\mathrm{M}_{\odot}\,\mathrm{pc}^{-2}\,\mathrm{Gyr}^{-1}$, for our best model with the non-linear Schmidt–Kennicutt law;
(ii) the infall time-scale for the gas mass growth of the MW disc is $\tau = 7\,\mathrm{Gyr}$;
(iii) the mass loading factor is $\omega = 0.4$.

Finally, the best models assume the single-degenerate scenario for the Type Ia SN rate. We remark on the fact that the predicted [Fe/H]-[O/Fe] relation in the MW is fitted by construction using fixed values for the key free parameters $\nu_{\rm L}$ (or SFR_0), ω and τ.

It is worth noting that the values of our best parameters are in agreement with previous recent studies (see e.g. Minchev, Chiappini & Martig 2013; Nidever et al. 2014; Spitoni et al. 2015); in particular, a typical infall time-scale $\tau \sim 7\,\mathrm{Gyr}$ and star formation efficiency $\sim 1\,\mathrm{Gyr}^{-1}$ are necessary to reproduce also the observed age-metallicity relation and the metallicity distribution function of the G-dwarf stars in the solar neighbourhood (Matteucci 2001, 2012; Pagel 2009).

Once the best set of free parameters is determined, we fix them and explore the effects of assuming different DTDs for the Type Ia SN rate and different prescriptions for the relation between the SFR and the surface gas mass density, $\sigma_{\rm gas}(r, t)$. In this way, we can demonstrate the flexibility of our method for solving the chemical evolution of galaxies by taking into account the major systematics in the theory.

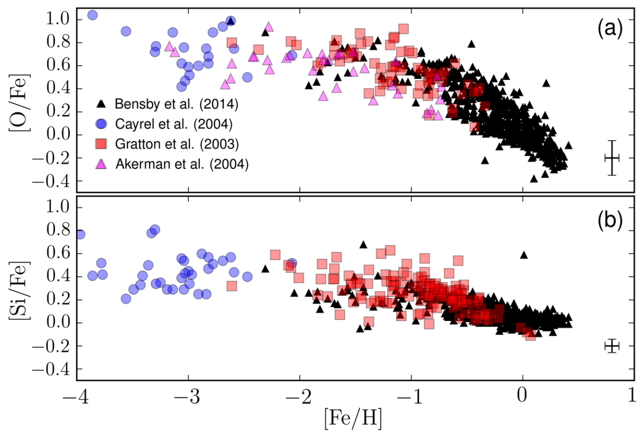

Figure 1. In this figure, we show the observed data set for the [O/Fe] (upper panel) and [Si/Fe] (bottom panel) versus [Fe/H] chemical abundance patterns that we assume in this work for the comparison with the predictions of our models. Data with different colours correspond to different works in the literature. In particular, our set of data for the solar neighbourhood includes MW halo stars from Gratton et al. (2003, red squares), Cayrel et al. (2004, blue circles) and Akerman et al. (2004, magenta triangles), and halo, thin and thick disc stars from Bensby, Feltzing & Oey (2014, black triangles).

3 THE OBSERVED DATA SET

The data set for the observed [Fe/H]–[O/Fe] and [Fe/H]–[Si/Fe] relations in the solar neighbourhood is shown in Fig. 1(a) and Fig. 1(b), respectively, where the data from different works are drawn with different colours. Our set of data includes both MW halo stars from Gratton et al. (2003, red squares), Akerman et al. (2004, magenta triangles) and Cayrel et al. (2004, blue circles), and MW halo, thin and thick disc stars from Bensby et al. (2014, black triangles).

The data in Fig. 1 span a wide metallicity range from $[\mathrm{Fe/H}] \approx -4.0$ dex to $[\mathrm{Fe/H}] \approx 0.5$ dex; they show a continuous trend in the [O/Fe] and [Si/Fe] abundance ratios as functions of the [Fe/H] abundances, although highly scattered. There is an initial, slowly decreasing plateau, followed by a steep decrease, which occurs at different [Fe/H] abundances and with different slopes when halo and disc stars are considered separately. This is particularly evident when looking at the [Si/Fe] ratios in Fig. 1(b), where the data of the halo stars by Gratton et al. (2003, red squares) decrease with a different slope with respect to the disc data by Bensby et al. (2014, black triangles).

In Fig. 2, we focus on the data set by Bensby et al. (2014) and show how the stars of the halo (magenta circles), thick disc (blue triangles) and thin disc (red triangles) are distributed in the [Fe/H]–[O/Fe] (upper panel) and [Fe/H]–[Si/Fe] (bottom panel) diagrams. Bensby et al. (2014) were able to assign a membership to the majority of the stars in their sample, according to the MW stellar component they likely belong to; in particular, Bensby et al. (2014) adopted a conservative kinematical criterion to retrieve the membership of the stars in their sample (see their appendix A). The presence of two well separate sequences between thin and thick disc stars, as suggested by many recent works in the literature (see e.g. Nidever et al. 2014; Kordopatis et al. 2015), is still not evident by

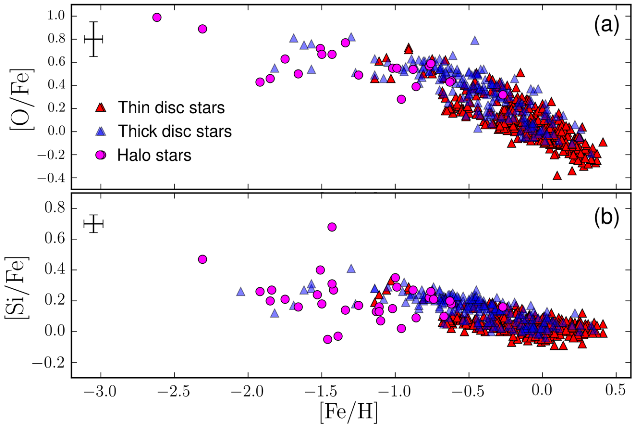

Figure 2. In this figure, we show how the stars at the solar neighbourhood in the Bensby et al. (2014) sample are distributed among the various MW stellar components. Halo stars are drawn as magenta circles; thick disc stars as blue triangles; finally, thin disc stars are shown as blue triangles. We remind the reader that Bensby et al. (2014) retrieve the membership of the stars in their sample with a kinematical criterion.

looking at the data set in Fig. 2, since the scatter is still relatively high. Nevertheless, the work by Bensby et al. (2014) claimed that thin and thick disc stars potentially exhibit two separate abundance trends, especially in the range of $-0.7 \lesssim$ [Fe/H] $\lesssim -0.35$ dex, expected by the authors also in the unpublished *Gaia* data.

4 RESULTS: THE MILKY WAY CHEMICAL EVOLUTION

In this section, we present the results of our chemical evolution model, which is based on the methods and equations as described in Section 2. We study the MW chemical evolution, with the aim of reproducing the observed [O/Fe] and [Si/Fe] abundance ratios as functions of the [Fe/H] abundance.

We first explore the effect of different prescriptions for the galaxy SFR. Successively, we investigate the effect of assuming different DTDs for Type Ia SNe.

4.1 Exploring the effect of different laws for the galaxy SFR

In Fig. 3, we compare the predictions of our best model with the linear Schmidt–Kennicutt law (solid lines in blue) with a similar model assuming a non-linear Schmidt–Kennicutt law. In particular, in Fig. 3(a), we show the predicted evolution of the galaxy SFR as a function of the galaxy lifetime; in Fig. 3(b), the predicted evolution of σ_{gas} with time; in Fig. 3(c), we show how the predicted star formation efficiency evolves as a function of time; finally, in Fig. 3(d), we show our results for the [O/Fe] versus [Fe/H] chemical abundance pattern.

By looking at Fig. 3(a), the predicted SFR is very similar when assuming the linear and the non-linear Schmidt–Kennicutt law, with similar absolute values for ν_{L} and SFR_0. The differences are always remarkable in the evolution of σ_{gas} with time [see Fig. 3(b)], particularly in the earliest stages of the galaxy evolution; in fact, the model with the non-linear Schmidt–Kennicutt law (dashed line in black) always predicts higher surface gas mass densities than the model with the linear Schmidt–Kennicutt law (solid blue line) for $t \lesssim 10$ Gyr. That can be explained by looking at Fig. 3(c), where we can appreciate that – for galaxy evolutionary times $t \lesssim 10$ Gyr – the model with the non-linear law has always higher SFEs [see equation (15)] than the model with the linear law, which has a fixed star formation efficiency $\nu = 2\,\mathrm{Gyr}^{-1}$. Since the predicted evolution of the galaxy SFR is very similar when assuming a linear or non-linear Schmidt–Kennicutt law, the differences in the predicted [O/Fe] versus [Fe/H] relation are negligible [see Fig. 3(d)].

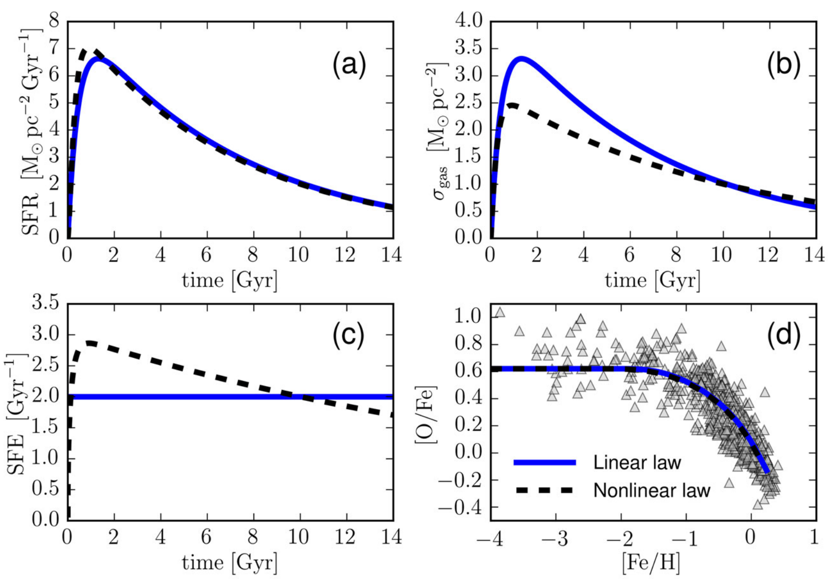

Figure 3. In this figure, we show the comparison between models with different prescriptions for the galaxy SFR. We examine a linear Schmidt–Kennicutt law [solid curves in blue; see equation (9)] and a non-linear Schmidt–Kennicutt law [dashed curves in black; see equation (14)]. In panel (a), we show the results for the evolution of the SFR as a function of time; in panel (b), we show how σ_{gas} is predicted to evolve with time; in panel (c), the temporal evolution of the star formation efficiency, defined as $\mathrm{SFE} = \psi(r,t)/\sigma_{\mathrm{gas}}(r,t)$, is drawn; finally, in panel (d), we show the evolutionary path of the models in the [Fe/H]–[O/Fe] diagram, with the grey triangles corresponding to the observed set of data for the stars in the solar neighbourhood (see Section 3). All the models assume fixed values of the key free parameters, in particular, $\nu_{\mathrm{L}} = 2\,\mathrm{Gyr}^{-1}$ (blue solid curves) and $\mathrm{SFR}_0 = 2\,\mathrm{M}_{\odot}\,\mathrm{pc}^{-1}\,\mathrm{Gyr}^{-1}$ (black dashed curves), infall time-scale $\tau = 7$ Gyr, mass loading factor $\omega = 0.4$ and the single-degenerate scenario for DTD of Type Ia SNe (see also Section 2.4 for the assumed set of free parameters).

The predicted evolutionary path of our models in the [Fe/H]–[O/Fe] diagram in Fig. 3(d) can be explained as follows by means of the so-called 'time delay model' (Tinsley 1979; Greggio & Renzini 1983; Matteucci & Greggio 1986).

(i) The plateau at very low [Fe/H] abundances stems from the chemical enrichment by massive stars, dying as core-collapse SNe, for which we assume IRA and hence a constant ratio between the net yields of oxygen and iron per stellar generation; in fact, in our simplified model, we do not assume the stellar yields of oxygen and iron per stellar generation to depend upon the metallicity (see also Vincenzo et al. 2016a).

(ii) The initial plateau is then followed by a decrease, which is due to the delayed contribution of Type Ia SNe, injecting large amounts of iron into the galaxy ISM. The position of the knee in the [Fe/H]–[O/Fe] relation is determined by the galaxy star formation efficiency. In particular, decreasing the star formation efficiency determines a slower production of iron and α-elements by massive stars and hence the decrease of the [O/Fe] ratios occurs at lower [Fe/H] abundances.

If we assumed the original Kennicutt (1998) law, which prescribes $\mathrm{SFR}_{0,\,\mathrm{K98}} = 2.5 \times 10^{-1}\,\mathrm{M}_{\odot}\,\mathrm{pc}^{-2}\,\mathrm{Gyr}^{-1}$, the star formation efficiencies – as defined by equation (15) – would be always roughly one order of magnitude lower than the findings of our best model, determining a decrease of the [O/Fe] ratios at very low [Fe/H] abundances, at variance with data.

4.2 Exploring the effect of different DTDs for Type Ia SNe

In Fig. 4, we show the effect of varying simultaneously the assumed DTDs for Type Ia SNe (curves with different colours in all the panels), and the prescriptions for the SFR law [Fig. 4(a1) and Fig. 4(a2) show the results of the models with the linear Schmidt–Kennicutt law for [O/Fe] and [Si/Fe] versus [Fe/H], respectively, while Figs 4(b1) and 4(b2) show the results for the law by Kennicutt (1998)].

By looking at Fig. 4, we can appreciate that different distributions of delay times for Type Ia SNe determine different behaviours of the models. Whatever is the assumed prescription for the galaxy SFR, the best agreement with the set of data for [O/Fe] versus [Fe/H] is achieved by the model with the single-degenerate scenario (blue solid lines), while the predicted trend of the [Si/Fe] versus [Fe/H] with the single-degenerate scenario is always above the data; such an offset for silicon is due to the still large uncertainty in the nucleosynthetic stellar yields of this chemical element.

The models with the bimodal DTD of Mannucci et al. (2006, dashed curves in black) predict a remarkable change in the behaviour of the declining trend of the [α/Fe] ratios, which is due to the assumed secondary population of Type Ia SNe, which contributes by 50 per cent to the global distribution of the delay times; this tardy component bolsters the iron pollution of the ISM at later times. Moreover, the [α/Fe] ratios with the bimodal DTD decline with the steepest slope among the assumed DTDs because of the too large number of prompt Type Ia SNe; this result is in agreement with the findings of Matteucci et al. (2006, 2009) and Yates et al. (2013); all these studies agree that the average number of prompt Type Ia SNe can vary from ∼15 per cent to a maximum of ∼30 per cent with respect to the integrated number of Type Ia SNe, hence a percentage which should be lower than the 50 per cent assumed by Mannucci et al. (2006), although these authors concluded that for their data also a percentage of 30 per cent could be acceptable. Finally, the models with the double-degenerate scenario (dashed–dotted red curves) predict a steeper declining trend of the

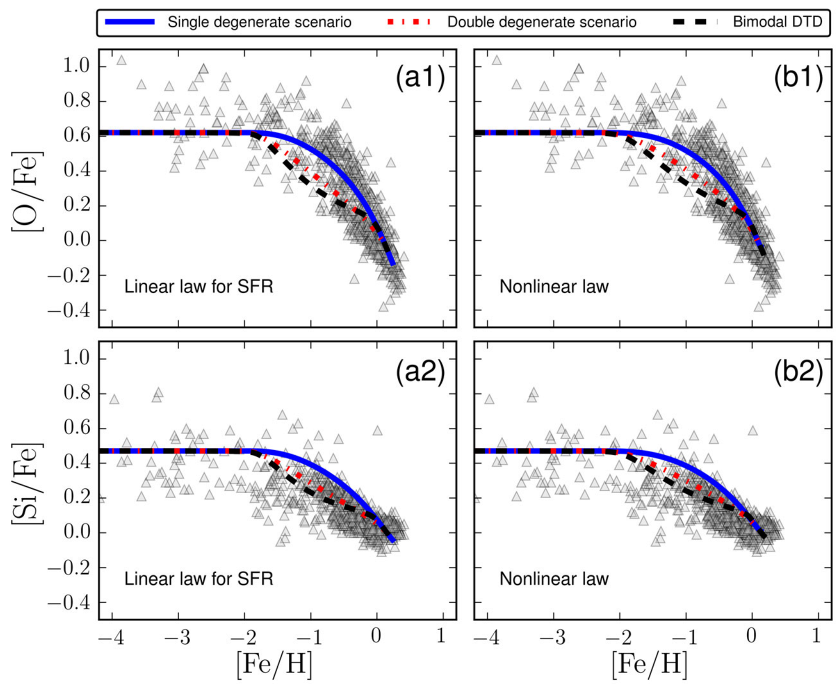

Figure 4. In this figure, we show the main results of our work for the [O/Fe] (upper panels) and [Si/Fe] (bottom panels) versus [Fe/H] chemical abundance patterns. Curves with different colours correspond to different assumptions for the DTD of Type Ia SNe. In this work, we examine the single-degenerate scenario (solid curves in blue), the double-degenerate scenario (dash–dotted red curves) and the bimodal DTD (dashed black curves). The panels (a1) and (a2) on the left show the predictions of the models with the linear Schmidt–Kennicutt law [see equation (9)], while the panels (b1) and (b2) on the right show the models with the non-linear Schmidt–Kennicutt law [see equation (14)].

[α/Fe] ratios than the single-degenerate scenario as first Type Ia SNe explode.

It is worth noting that, if there are separate sequences for thick and thin disc stars, then the double-degenerate DTD (and even the unlikely bimodal DTD) may provide a better fit to the MW thin disc than the single-degenerate scenario, within our simplified model.

5 CONCLUSIONS AND DISCUSSION

In this work, we have presented a new theoretical framework for following the chemical evolution of galaxies by assuming IRA for chemical elements synthesized and restored by massive stars on short typical time-scales and the DTD formalism for the delayed chemical enrichment by Type Ia SNe. The main assumptions of our model are the galaxy gas mass assembly history, the stellar yields and the IMF. Finally, the SFR law also represents another fundamental phenomenological assumption in the model.

We have derived a very simple and general formula (equation 11), relating the Laplace transform of the galaxy SFH with the Laplace transform of the galaxy gas mass assembly history, provided the galaxy SFR follows a linear Schmidt–Kennicutt law, namely $\psi(r, t) \propto \sigma_{\rm gas}(r, t)$. This formula can be used both to derive the galaxy SFH from the assumed gas infall law and to solve the corresponding inverse problem (i.e. retrieving the galaxy gas accretion history from the observed SFH). We remark on the fact that the Laplace transform method for solving ordinary differential equations can be used when the latter are linear in the unknown.

In this work, we have also considered the case of a non-linear ordinary differential equation for the evolution of the galaxy surface gas mass density with time, which can be obtained by assuming $\psi(r, t) \propto \sigma_{\rm gas}(r, t)^k$, with $k = 1.4$ (nonlinear Schmidt-Kennicutt law, with same same index k as given in Kennicutt 1998). In this case, the equation has been solved numerically; then, the derived galaxy SFH has been assumed as an input for the chemical evolution model.

We have shown that the differential equation for the evolution of a generic chemical element X can be solved with standard numerical methods (e.g. the Runge–Kutta algorithm), once the galaxy SFH has been theoretically determined from our assumptions. We have applied our model to reproduce the [O/Fe] and [Si/Fe] versus [Fe/H] chemical abundance patterns as observed in the solar neighbourhood by exploring the effect of different DTDs for Type Ia SNe and different prescriptions for the SFR law. We have assumed the Galaxy disc to assemble by means of a single gas accretion episode, with typical time-scale $\tau = 7$ Gyr. In any case, our method can be easily extended also for a two-infall model (Chiappini, Matteucci & Gratton 1997).

Our model with the single-degenerate scenario for Type Ia SNe provides a very good agreement with the observed [Fe/H]–[O/Fe] relation in the MW. Since the nucleosynthetic stellar yields of the other α-elements, like Si, Ca or Mg, still suffer from large uncertainty, the agreement between model and data for these chemical elements is still not good. We also conclude that, if there are two separate sequences between thin and thick disc data, then our models with the double-degenerate scenario (or even the bimodal DTD) may provide a better fit to the thin disc data.

We remark on the fact that a linear relation between the SFR and $\sigma_{\rm gas}$ seems not to be the best fit to data, unless the star formation efficiency is defined as the inverse of the typical dynamical time-scale of the system. Nevertheless, we have shown that our models with a non-linear Schmidt–Kennicutt law provide very similar results for the galaxy SFH and chemical abundance patterns as the model with the linear Schmidt–Kennicutt law.

We are aware that the assumption of a constant yield per stellar generation is a strong approximation, determining the predicted flat trend of the [α/Fe] ratios at low [Fe/H] abundances at variance with data showing a remarkable scatter. This scatter can be reproduced only by introducing an element of stochasticity in the model (e.g. in the stellar yields, in the IMF or in the SFR). Moreover, the [α/Fe] ratios at very low [Fe/H] abundances show a global trend, which can be reproduced only by relaxing IRA, and hence by including stellar lifetimes and variable nucleosynthetic stellar yields of massive stars, as in the detailed numerical codes of chemical evolution. As Type Ia SNe start exploding, the [α/Fe] ratios steeply decrease in excellent agreement with data.

The theoretical method, as presented in this work, differs from previous works in the literature, which similarly recover the galaxy chemical evolution from the assumed SFH (see e.g. Erb et al. 2006; Homma et al. 2015; Weinberg et al. 2016), because we initially start from the assumption of a galaxy gas mass assembly history. Then, the galaxy SFH has been retrieved either by means of equation (11), which makes use of the Laplace transform to simplify the solution of the differential equation for the evolution of the galaxy gas mass, or by means of numerical techniques. Our theoretical framework can be generalized for any choice of the galaxy gas infall law.

Our method for solving chemical evolution of galaxies can be easily included in other complementary stellar population synthesis models by taking into account chemical elements – like iron – which are restored with a time delay from the star formation event. In this way, one can easily decouple the evolution of iron and oxygen, which contributes to the total metallicity of the galaxy ISM with different relative fractions as a function of the galaxy lifetime.

ACKNOWLEDGEMENTS

We thank S. Recchi and F. Belfiore for their remarks upon reading the manuscript and for insightful discussions; we also thank two anonymous referees for their suggestions and constructive comments. FM and ES acknowledge funding from PRIN-MIUR 2010-2011 project 'The Chemical and Dynamical Evolution of the Milky Way and Local Group Galaxies', prot. 2010LY5N2T.

REFERENCES

Akerman C. J., Carigi L., Nissen P. E., Pettini M., Asplund M., 2004, A&A, 414, 931
Bell E. F., McIntosh D. H., Katz N., Weinberg M. D., 2003, ApJS, 149, 289
Bensby T., Feltzing S., Oey M. S., 2014, A&A, 562, A71
Bigiel F., Leroy A., Walter F., Brinks E., de Blok W. J. G., Madore B., Thornley M. D., 2008, AJ, 136, 2846
Bigiel F. et al., 2011, ApJ, 730, L13
Boissier S., Prantzos N., 2000, MNRAS, 312, 398
Bressan A., Chiosi C., Fagotto F., 1994, ApJS, 94, 63
Brocato E., Matteucci F., Mazzitelli I., Tornambe A., 1990, ApJ, 349, 458
Calura F., Lanfranchi G. A., Matteucci F., 2008, A&A, 484, 107
Calura F., Ciotti L., Nipoti C., 2014, MNRAS, 440, 3341
Cassarà L. P., Piovan L., Chiosi C., 2015, MNRAS, 450, 2231
Cayrel R. et al., 2004, A&A, 416, 1117
Chiappini C., Matteucci F., Gratton R., 1997, ApJ, 477, 765
Chiosi C., 1980, A&A, 83, 206
Erb D. K., Steidel C. C., Shapley A. E., Pettini M., Reddy N. A., Adelberger K. L., 2006, ApJ, 646, 107
Faucher-Giguère C. A., Kereš D., Ma C. P., 2011, MNRAS, 417, 2982
Genzel R. et al., 2010, MNRAS, 407, 2091
Gibson B. K., 1997, MNRAS, 290, 471
Gratton R. G., Carretta E., Claudi R., Lucatello S., Barbieri M., 2003, A&A, 404, 187

Greggio L., 2005, A&A, 441, 1055
Greggio L., Renzini A., 1983, Mem. Soc. Astron. Ital., 54, 311
Homma H., Murayama T., Kobayashi M. A. R., Taniguchi Y., 2015, ApJ, 799, 230
Iwamoto K., Brachwitz F., Nomoto K., Kishimoto M., Umeda H., Hix W. R., Thielemann F.-K., 1999, ApJS, 125, 439
Kennicutt R. C., Jr, 1998, ApJ, 498, 541
Kordopatis G. et al., 2015, A&A, 582, A122
Kroupa P., Tout C. A., Gilmore G., 1993, MNRAS, 262, 545
Kuijken K., Gilmore G., 1991, ApJ, 367, L9
Larson R. B., 1976, MNRAS, 176, 31
Leroy A. K., Walter F., Brinks E., Bigiel F., de Blok W. J. G., Madore B., Thornley M. D., 2008, AJ, 136, 2782
Maeder A., 1992, A&A, 264, 105
Mannucci F., Della Valle M., Panagia N., 2006, MNRAS, 370, 773
Maoz D., Mannucci F., Nelemans G., 2014, ARA&A, 52, 107
Matteucci F., 2001, Astrophysics and Space Science Library, Vol. 253, The Chemical Evolution of the Galaxy. Kluwer, Dordrecht, p. 293
Matteucci F., 2012, Chemical Evolution of Galaxies. Springer-Verlag, Berlin
Matteucci F., Greggio L., 1986, A&A, 154, 279
Matteucci F., Recchi S., 2001, A&A, 558, 351
Matteucci F., Panagia N., Pipino A., Mannucci F., Recchi S., Della Valle M., 2006, MNRAS, 372, 265
Matteucci F., Spitoni E., Recchi S., Valiante R., 2009, A&A, 501, 531
Micali A., Matteucci F., Romano D., 2013, MNRAS, 436, 1648
Minchev I., Chiappini C., Martig M., 2013, A&A, 558, A9
Nidever D. L. et al., 2014, ApJ, 796, 38
Pagel B. E. J., 2009, Nucleosynthesis and Chemical Evolution of Galaxies, 2nd edn. Cambridge Univ. Press, Cambridge
Ruiz-Lapuente P., Canal R., 1998, ApJ, 497, L57
Schönrich R., Binney J., 2009, MNRAS, 396, 203
Schruba A. et al., 2011, AJ, 142, 37
Silk J., 1997, ApJ, 481, 703
Silva L., Granato G. L., Bressan A., Danese L., 1998, ApJ, 509, 103
Spitoni E., Romano D., Matteucci F., Ciotti L., 2015, ApJ, 802, 129
Spitoni E., Vincenzo F., Matteucci F., 2016, preprint (arXiv:1605.05603)
Strolger L. G. et al., 2004, ApJ, 613, 200
Talbot R. J., Jr, Arnett W. D., 1975, ApJ, 197, 551
Tinsley B. M., 1979, ApJ, 229, 1046
Tinsley B. M., 1980, Fundam. Cosm. Phys., 5, 287
Totani T., Morokuma T., Oda T., Doi M., Yasuda N., 2008, PASJ, 60, 1327
Vincenzo F., Matteucci F., Belfiore F., Maiolino R., 2016a, MNRAS, 455, 4183
Vincenzo F., Matteucci F., de Boer T. J. L., Cignoni M., Tosi M., 2016b, MNRAS, 460, 2238
Weinberg D. H., Andrews B. H., Freudenburg J., 2016, preprint (arXiv:1604.07435)
Yates R. M., Henriques B., Thomas P. A., Kauffmann G., Johansson J., White S. D. M., 2013, MNRAS, 435, 3500

This paper has been typeset from a TEX/LATEX file prepared by the author.